JOTCS A
Journal of the Turkish Chemical Society
Section: A
Chemistry
TURKISH CHEMICAL SOCIETY

Photo-Induced Tautomerism of Isocytosine in Aqueous Solution when Irradiated with UVC Light

Tsvetina D. Cherneva, Mina M. Todorova, Rumyana I. Bakalska, Vassil B. Delchev*

University of Plovdiv, Faculty of Chemistry, Department of Chemistry, Plovdiv, 4000, Bulgaria

Abstract: It was found that the irradiation of aqueous solution of isocytosine with UVC light provokes an oxo-hydroxy phototautomerism of the compound with a rate constant of 5.29×10^{-3} min^{-1}. It was observed a backward reaction, after removing the UV light source, with a rate constant of 0.12×10^{-3} min^{-1}. Two mechanisms of the phototautomerism were investigated at the B3LYP/aug-cc-pVDZ theoretical level in water surroundings (PCM). The first one showed a consecutive dissociation and association of a proton through conical intersections S_0/S_1 whose structures were located at the same theoretical level in the gas phase. It occurs along the $^1\pi\sigma^*$ excited-state reaction pathway. The more probable mechanism includes an excited-state H-transfer supported by a water molecule as a catalyst. It occurs along the $^1\pi\pi^*$ excited-state reaction pathway which we found over the IRC ground-state energy curve. The water molecule drastically reduces the energy barrier in the ground state as well in the excited state.

Keywords: Conical intersections S_0/S_1, Excited states, Isocytosine, TD DFT methods, UV irradiation.

Submitted: July 11, 2023. **Accepted:** December 11, 2023.

Cite this: Cherneva TD, Todorova MM, Bakalska RI, Delchev VB. Photo-Induced Tautomerism of Isocytosine in Aqueous Solution when Irradiated with UVC Light. JOTCSA. 2024; 11(1): 321-30.

DOI: https://doi.org/10.18596/jotcsa.1325480.

***Corresponding author. E-mail:** vdelchev@uni-plovdiv.net

1. INTRODUCTION

Nucleobases are major chromophores in macromolecules of DNA and RNA (1-4). It is known they are photostable compounds (5-8) since they absorb and utilize the UV light as in this way they prevent the normal functioning of the nucleic acids. The high photostabiliy of pyrimidine bases leads to another question namely why their close analogues do not exhibit such features!

One analogue of nucleobase cytosine is isocytosine. The two compounds differ only by the positions of the functional groups NH_2 and C=O – they have exchanged positions in the two analogues. However, cytosine is known to be photostable whereas isocytosine is not (9-11).

Isocytosine is known as a “rare” nucleobase because of its very low frequency of distribution in the macromolecules of nucleic acids. Despite that there is an experimental evidence for investigations of isocytosine pairing with isoguanine in the helix of DNA (12,13). Moreover isocytosine has been tested for an application for the treatment of Alzheimer’s disease (14,15).

Jeffrey has studied the crystal structure of isocytosine and has proposed the next unit cell parameters: a=8.745 Å, b=11.412 Å, c=10.414 Å, β=94.79°, with a space group $P2_1/n$ and unit cell volume V=1038 A^3 for multiplicity Z=8 (16,17).

Isocytosine exists in two oxo tautomers which are available in aqueous solution (18-21). However, Vranken (22) has reported for some other tautomers which are formed when matrix isolated isocytosine is irradiated with UV light (λ_{max}=308 nm) about 45 min. The analysis of the IR spectra of the photoproducts has shown OH stretching vibrations which come from the hydroxy tautomers of isocytosine. The ratio of the concentrations of the oxo and hydroxy tautomers is [oxo]/[hydroxy] = 0.11 (23). Recently we reported on the irradiation of

acetonitrile solution of isocytosine (λ_{max}= 330 nm, for 60 min). It was established an oxo → hydroxy tautomerism (10). Unfortunately, the mechanism of this tautomeric conversion is not well documented especially when a water molecule is engaged in the excited-state proton transfer process. The role of the water molecule from the solution can be regarded as a catalyst of the photoreaction.

The tautomerism in pyrimidines has been explained by the PIDA (photo-induced dissociation association) mechanism (24,25) and it has been shown that the driven state is the repulsive $^1\pi\sigma^*$ excited state (26-28). However, when a water molecule is attached to the H-atoms which should be detached the dissociation of the proper N-H/O-H bond should occur by another mechanism, different from PIDA.

The aim of the current research is to through light upon the mechanism of the excited state proton transfer process oxo → hydroxy in isocytosine. Two mechanisms are tested – PIDA and IRC with a water molecule. The importance of the research comes from the experimental fact that pyrimidine nucleobases are photostable compounds whereas their analogues usually are not. Such research would answer partially to the question why the nature “has chosen” cytosine to be a chromophore present in nucleic acid macromolecules and not isocytsine.

2. THEORETICAL METHODS

The ground-state equilibrium geometries of several tautomers of isocytosine were optimized at the B3LYP/aug-cc-pVDZ and CC2/aug-cc-pVDZ levels in the gas phase and in water medium (only for the DFT calculations). The calculation at the DFT level involves the Becke (29) 3-parameter and Lee–Yang–Parr (30) exchange-correlation functional. The CC2 calculations are based on coupled cluster methods (31).

Subsequent frequency calculations were performed to prove that the found structures are located in minima on the corresponding PESs. No imaginary frequencies were calculated for all geometries. The equilibrium geometries were used to compute the vertical excitation energies at the TD DFT (32,33) and CC2 (31) theoretical levels.

In order to study the water assisted H-transfer we optimized, at the B3LYP/aug-cc-pVDZ and water surroundings (PCM, polarized continuum model (34)), the structures of selected H-bonded complexes of tautomers of isocytosine with one water molecule. The transition state of the intermolecular proton transfer was found with one imaginary frequency whose form describes the H-motion between the proper centres in order to form a stable H-bonded complex. Using the IRC structures standing between the initial complex and the complex-product we followed the excited-state reaction paths of the tautomeric process.

The conical intersections S_0/S_1 connected with the elongation of the corresponding N-H and O-H bonds in the tautomers were optimized at the B3LYP/aug-cc-pVDZ level of theory in the gas phase. The structures were used for linear interpolation in internal coordinates (LIIC) with the geometries minima. The linear interpolation was performed by the equation:

$$Q_i = Q_i(I) + \varepsilon.[Q_i(F) - Q_i(I)] \quad (1)$$

where $Q_i(I)$ is the i-th coordinate of the initial structure (tautomer – minimum); $Q_i(F)$ is the same coordinate of the final structure (conical intersection S_0/S_1 in this case); ε is the interpolation parameter, which changes in the interval 0 (initial structure) ÷ 1 (final structure). It means that the interpolation parameter ε can be treated as a reaction coordinate of the—mechanism under study. The vertical excitation energies of the structures along the reaction coordinate were computed at the TD B3LYP/aug-cc-pVDZ level in order to get the excited-state reaction paths of the H-detachment processes.

All calculations–were performed with the GAUSSIAN 16 software (35). The conical intersections S_0/S_1 were found with the GAMESS-US program (36).

3. EXPERIMENTAL METHODS

The experiment includes a preparation of aqueous solution of isocytosine (Sigma-Aldrich) with concentration 1.3×10^{-4} mol.L^{-1}. The solution was deaerated with nitrogen for 15 min to turn out of the air. After that the solution was irradiated in a standard photochemical reactor (220 cm^3) with a low pressure mercury lamp TNN 15/32 (Hanau Original) emitting light at λ_{max} = 254 nm. Samples with volume of 3 cm^3 were taken in 10 min intervals for registering of the UV absorption spectra and following the changes in the mixture in the course of the irradiation. After removing the UV light source, the changes of the reaction mixture in dark were checked out in 60 min intervals. The UV spectra were recorded on an Agilent Cary 60 UV/Vis spectrophotometer, double beam, and spectral range of 190 – 1100 nm.

4. RESULTS AND DISCUSSIONS

4.1. Ground-state equilibrium geometries and conical intersections S_0/S_1

The ground-state equilibrium geometries of isocytosine tautomers optimized in water surroundings (PCM) are illustrated in Figure 1. Two oxo-amino tautomers are included in the research – iC_A and iC_D. The pyramidal character of the amino group of these tautomers could be estimated by the sum of the bond angles (Σ) around N_7 and its deviation (δ) from 360°. For oxo-amino forms iC_A and

iC_D the Σ values are 355.5° and 358.1°, whereas the δ quantities are 4.5° and 1.9° correspondingly. It means that the pyramidal character is more pronounced in tautomers iC_A. The amino group in the oxo-amino form iC_D is in a greater degree conjugated with the aromatic ring. In tautomer iC_E the pyramidal character of the amino group is the most pronounced: Σ = 355.1° and δ = 4.9°.

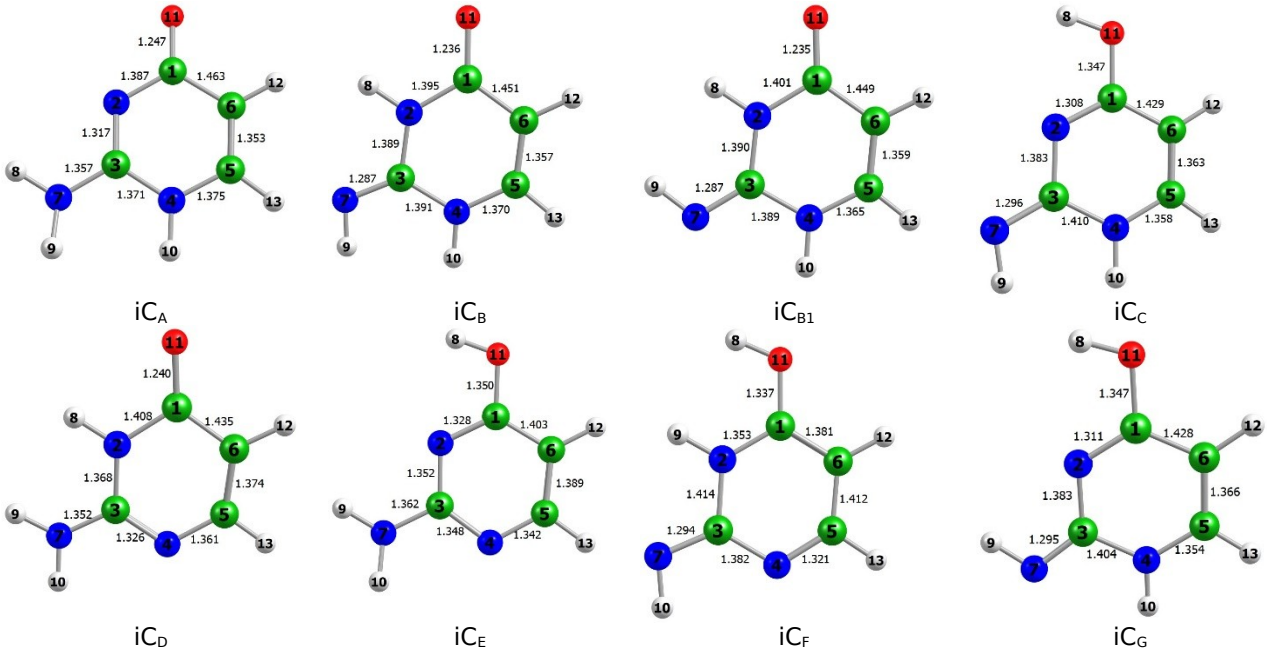

Figure 1: Ground-state equilibrium geometries of isocytosine tautomers in water environment (B3LYP/aug-cc-pVDZ and PCM).

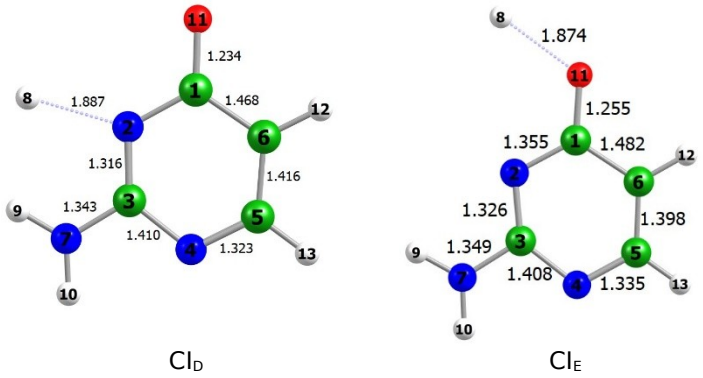

Figure 2: Optimized conical intersections S_0/S_1 of tautomers iC_D and iC_E at the B3LYP/aug-cc-pVDZ in the gas phase.

The structure of two conical intersections S_0/S_1 of tautomers iC_D and iC_E connected with elongation of the N_2-H and O_{11}-H bonds are illustrated in Figure 2. As seen the dissociations of the corresponding bonds occur in the molecular plane. The amino groups in the two structures are completely conjugated with the aromatic rings which can be deduced by the Σ values: both are equal to 360° (δ = 0°). These structures are used further for linear interpolation in internal coordinates.

4.2. Vertical excitation energies and experimental UV absorption spectra

The calculated vertical excitation energies of all tautomers of isocytosine are listed in Table 1. The first excited state of all tautomers, except iC_A is the spectroscopically bright $^1\pi\pi^*$ electronic state. Only for the oxo-amino tautomer iC_A the first excited state calculated at the B3LYP/aug-cc-pVDZ theoretical level is the dark $^1n\pi^*$ one. According to the TD B3LYP computations the $^1\pi\sigma^*$ excited states of the two oxo-amino tautomers iC_A and iC_D in the gas phase have lower energies (~4.9 eV) than in aqueous medium (more than 5.3 eV). With regards to the PIDA mechanism (24,25) in water medium this driven state should be populated with a lower probability than in the gas phase.

In order to assign the available tautomers in the non-irradiated and irradiated aqueous solution of

isocytosine we simulated the theoretical spectra of all tautomers. We found that only the simulated spectra of tautomers iC_D and iC_E in a largest degree fit to the experimental UV curves. They are illustrated in Figure 3. The experimental spectrum of the non-irradiated solution shows an insignificant shoulder at about 227 nm which corresponds to the $\pi\rightarrow\pi^*$ electron transition of tautomer iC_D. Furthermore, a $\pi\rightarrow\pi^*$ electron transition of the same tautomer is the origin of the maximum at 285 nm. In the course of the irradiation is decreases the absorption and transforms into a shoulder whose origin is the $\pi\rightarrow\pi^*$ electron transition in tautomer iC_E. The shoulder at 227 nm gets more structured and starts to shape a peak which could be assigned to the $\pi\rightarrow\pi^*$ electron transition of tautomer iC_E. The experimental spectrum of the non-irradiated solution in Figure 3 shows also a presence of oxo-amino tautomer iC_A. The two most intensive absorption maxima were assigned to be for the $^1\pi\pi^*$ excited states.

Table 1: Vertical excitation energies – B3LYP/aug-cc-pVDZ and CC2/aug-cc-pVDZ. Oscillator strength f.10^2 (in Italic).

iC_A						iC_B					
1				**2**		**1**				**2**	
water		gas		gas		water		gas		gas	
	eV		eV		eV		eV		eV		eV
$^1n\pi^*$	4.671	$^1n\pi^*$	4.215	$^1\pi\pi^*$	4.260	$^1\pi\pi^*$	4.456	$^1\pi\pi^*$	4.508	$^1\pi\pi^*$	4.722
	0.02		*0.01*		*0.01*		*7.44*		*4.14*		*0.0*
$^1\pi\pi^*$	5.192	$^1n\pi^*$	4.808	$^1\pi\pi^*$	4.797	$^1n\pi^*$	4.926	$^1n\pi^*$	4.621	$^1\pi\pi^*$	4.852
	6.27		*0.08*		*0.13*		*0.00*		*0.00*		*8.23*
$^1n\pi^*$	5.409	$^1\pi\sigma^*$	4.912	$^1\pi\sigma^*$	4.927	$^1\pi\sigma^*$	5.389	$^1\pi\sigma^*$	4.883	$^1\pi\sigma^*$	5.070
	0.15		*0.04*		*0.32*		*1.16*		*0.28*		*0.35*
$^1\pi\pi^*$	5.519	$^1n\sigma^*$	4.922	$^1\pi\pi^*$	5.231	$^1\pi\pi^*$	5.673	$^1\pi\pi^*$	5.560	$^1\pi\pi^*$	5.760
	3.41		*0.13*		*3.37*		*19.21*		*9.82*		*12.73*
$^1\pi\sigma^*$	5.699	$^1\pi\pi^*$	5.141	$^1\pi\sigma^*$	5.258	$^1\pi\pi^*$	5.926	$^1\pi\sigma^*$	5.772	$^1\pi\sigma^*$	5.979
	0.97		*3.30*		*3.81*		*30.08*		*0.01*		*0.01*
iC_{B1}						iC_C					
1				**2**		**1**				**2**	
water		gas		gas		water		gas		gas	
	eV		eV		eV		eV		eV		eV
$^1\pi\pi^*$	4.434	$^1\pi\pi^*$	4.474	$^1\pi\pi^*$	4.748	$^1\pi\pi^*$	4.017	$^1\pi\pi^*$	3.891	$^1\pi\pi^*$	4.043
	8.48		*5.76*		*11.73*		*3.82*		*2.38*		*3.38*
$^1n\pi^*$	4.888	$^1n\pi^*$	4.636	$^1n\pi^*$	4.758	$^1\pi\sigma^*$	5.094	$^1\pi\sigma^*$	4.531	$^1\pi\sigma^*$	4.667
	0.00		*0.00*		*0.02*		*1.19*		*0.32*		*0.36*
$^1\pi\sigma^*$	5.395	$^1\pi\sigma^*$	5.126	$^1\pi\sigma^*$	5.297	$^1n\pi^*$	5.289	$^1n\pi^*$	4.887	$^1n\pi^*$	5.213
	1.27		*0.51*		*0.67*		*0.19*		*0.06*		*0.17*
$^1\pi\pi^*$	5.688	$^1\pi\sigma^*$	5.581	$^1\pi\sigma^*$	5.792	$^1\pi\sigma^*$	5.591	$^1n\pi^*$	5.264	$^1\pi\sigma^*$	5.590
	22.01		*0.17*		*0.17*		*0.01*		*0.08*		*0.24*
$^1\pi\sigma^*$	5.889	$^1\pi\pi^*$	5.612	$^1\pi\pi^*$	5.846	$^1\pi\pi^*$	5.599	$^1\pi\sigma^*$	5.370	$^1n\pi^*$	5.609
	0.01		*10.82*		*11.21*		*34.78*		*0.24*		*0.04*
iC_D						iC_E					
1				**2**		**1**				**2**	
water		gas		gas		water		gas		gas	
	eV		eV		eV		eV		eV		eV
$^1\pi\pi^*$	4.607	$^1\pi\pi^*$	4.629	$^1\pi\pi^*$	4.614	$^1\pi\pi^*$	4.750	$^1\pi\pi^*$	4.814	$^1\pi\pi^*$	4.768
	21.41		*14.69*		*18.50*		*8.77*		*6.84*		*8.08*
$^1n\pi^*$	5.072	$^1n\pi^*$	4.814	$^1n\pi^*$	4.820	$^1n\pi^*$	5.008	$^1n\pi^*$	4.942	$^1n\pi^*$	5.081
	0.01		*0.00*		*0.08*		*0.38*		*0.30*		*0.40*
$^1\pi\sigma^*$	5.339	$^1\pi\sigma^*$	4.897	$^1\pi\sigma^*$	5.300	$^1\pi\sigma^*$	5.485	$^1\pi\sigma^*$	5.312	$^1\pi\sigma^*$	5.567
	0.78		*1.15*		*0.89*		*1.18*		*1.07*		*2.14*
$^1n\pi^*$	5.476	$^1n\pi^*$	5.381	$^1n\pi^*$	5.658	$^1\pi\pi^*$	5.713	$^1n\pi^*$	5.654	$^1n\pi^*$	5.829
	0.02		*0.01*		*0.05*		*27.00*		*0.18*		*1.26*
$^1\pi\pi^*$	5.756	$^1\pi\sigma^*$	5.756	$^1n\sigma^*$	5.925	$^1n\pi^*$	5.721	$^1\pi\sigma^*$	5.701	$^1\pi\pi^*$	5.849
	17.57		*0.87*		*9.42*		*3.49*		*1.66*		*26.57*
iC_F						iC_G					
1				**2**		**1**				**2**	
water		gas		gas		water		gas		Gas	

	eV		eV		eV		eV		eV		eV
$^1\pi\pi^*$	3.861	$^1\pi\pi^*$	3.784	$^1\pi\pi^*$	3.750	$^1\pi\pi^*$	3.970	$^1\pi\pi^*$	3.820	$^1\pi\pi^*$	3.926
	8.50		*5.61*		*8.71*		*3.79*		*2.48*		*3.66*
$^1\pi\sigma^*$	4.890	$^1\pi\sigma^*$	4.139	$^1\pi\sigma^*$	4.520	$^1\pi\sigma^*$	5.120	$^1\pi\sigma^*$	4.770	$^1\pi\sigma^*$	4.927
	0.42		*0.00*		*0.03*		*1.26*		*0.45*		*0.57*
$^1n\pi^*$	4.924	$^1n\pi^*$	4.690	$^1n\pi^*$	4.870	$^1n\pi^*$	5.400	$^1n\pi^*$	5.105	$^1n\pi^*$	5.458
	0.22		*0.14*		*0.20*		*0.15*		*0.00*		*0.07*
$^1\pi\sigma^*$	5.402	$^1n\pi^*$	5.113	$^1\pi\sigma^*$	5.371	$^1\pi\sigma^*$	5.574	$^1\pi\sigma^*$	5.252	$^1\pi\sigma^*$	5.591
	0.78		*0.22*		*1.11*		*0.02*		*0.04*		*0.11*
$^1n\pi^*$	5.450	$^1\pi\sigma^*$	5.197	$^1n\pi^*$	5.447	$^1\pi\pi^*$	5.589	$^1n\pi^*$	5.315	$^1n\pi^*$	5.609
	0.17		*0.82*		*0.28*		*35.95*		*0.30*		*0.54*

1: B3LYP/aug-cc-pVDZ; **2**: CC2/aug-cc-pVDZ.

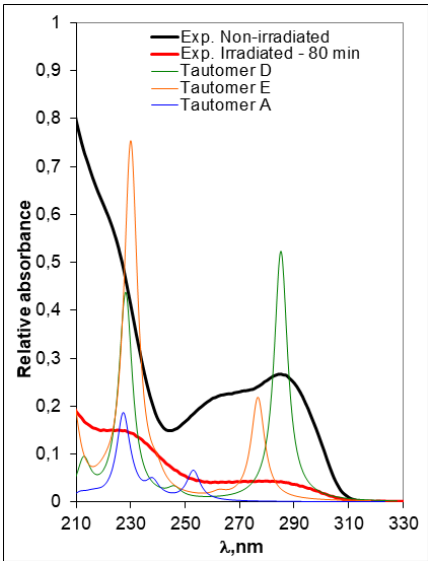

Figure 3: Experimental and theoretical spectra of isocytosine. The experimental spectra are for not-irradiated and irradiated (80 min) aqueous solutions of the compound. The theoretical spectra were simulated with a Lorentzian broadening of the bands. The theoretical spectra (B3LYP/aug-cc-pVDZ) are scaled with a scale factor of 1.06.

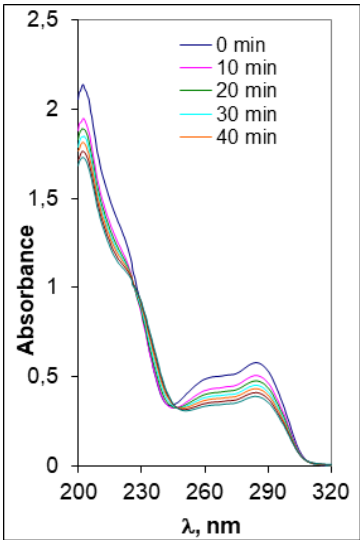

Figure 4: UV spectra of irradiated aqueous solution of isocytosine at different irradiation times.

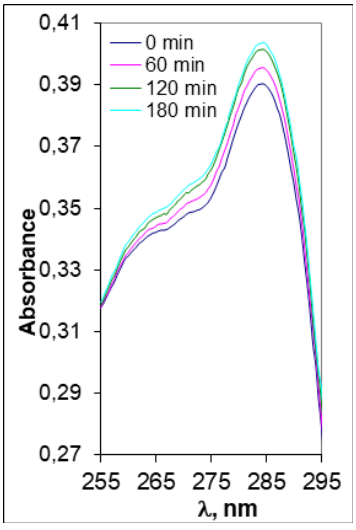

Figure 5: UV spectra of the aqueous solution of isocytosine after removing the UV light source (reaction in dark).

In Figure 4 are presented the UV spectra of the irradiated aqueous solution of isocytosine at different irradiation times. The spectra show regular decrease of the maxima at 285 nm and 202-203 nm. Using the first maximum we calculated the rate constant of the photoreaction which is 5.29×10^{-3} min^{-1}. The order of the reaction (first) implies a tautomeric process. The analysis of the UV spectra reveals that it should be a transformation of tautomer iC_D into hydroxy form iC_E.

We also followed the kinetics of the dark (thermal) reaction after removing the UV light source. It is observed in Figure 5 a slight restoration of the initial positions of the peaks as before the irradiation. It means that the tautomerization goes back thermally (in the ground state) and leads to the formation of the stable iC_D oxo-amino form. The calculated rate constant of the "dark" reaction ~~of~~ is 0.12×10^{-3} min^{-1} and it indicates that the thermal reaction is 44 times slower than the photochemical one.

4.3. Excited-state reaction pathways

LIIC pathways

We performed linear interpolation in internal coordinates in three stages: i) interpolation between tautomers iC_D and the conical intersection CI_D; ii) interpolation between the two conical intersections CI_D and CI_E; iii) interpolation between the conical intersection CI_E and tautomers iC_E. The results are summarized in Figure 6. As seen the ground-state energy barrier of the transformation $iC_D \rightarrow iC_E$ is very high - 5.732 eV. Along the $^1\pi\sigma^*$ excited-state reaction path the tautomerization can occur through a much lower energy barrier of 0.535 eV. Moreover, the $^1\pi\sigma^*$ excited-state reaction curve shows two clear minima where the excited system can be trapped. In the reaction interval $iC_D \rightarrow CI_D$ the photoreaction could prolong towards the stabilization of the ground state of the initial tautomer (iC_D) through internal conversion. In other words, two competitive reactions are expected: the phototautomerism of iC_D into iC_E and stabilization of tautomer iC_D through internal conversion. This fact agrees well with the low value of the rate constant of the photoreaction given above.

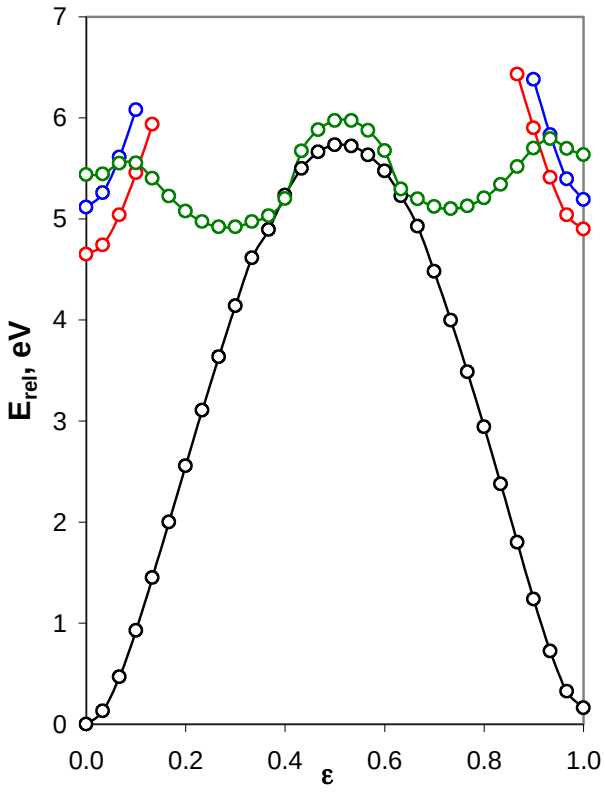

Figure 6: Linearly-interpolated excited-state reaction paths of the transformation $iC_D \rightarrow CI_D \rightarrow CI_E \rightarrow iC_E$, found at the B3LYP/aug-cc-pVDZ theoretical level in water surroundings (PCM). The relative energy was calculated according to the energy of tautomer iC_D (-395.012484 a.u.)

Excited-state water-assisted proton transfer

In order to apply the IRC approach for the study of the tautomerism $iC_D \rightarrow iC_E$ we oprimized the H-bonded-complexes of tautomers iC_D and iC_E and the ground state transition state located between them. Their structures are given in Figure 7.

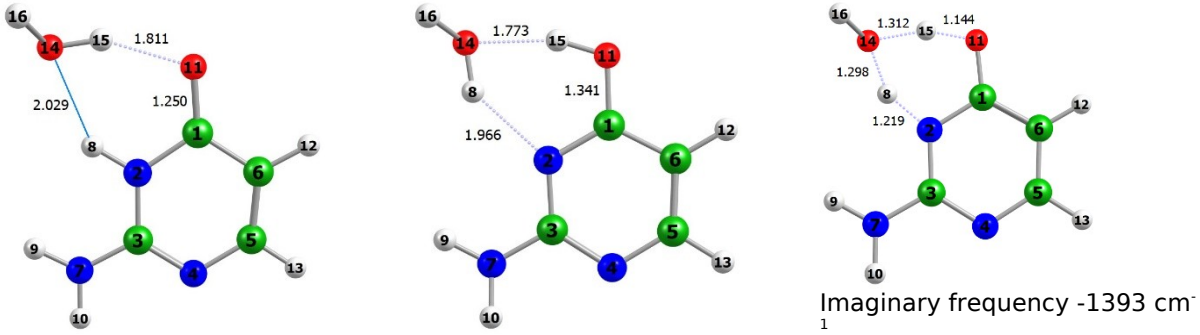

iC_{DW} iC_{EW} Transition state

Figure 7: H-bonded complexes of iC_D and iC_E and the transition state of their mutual interconversion, all found at the B3LYP/aug-cc-pVDZ level in water surroundings (PCM).

The transition state has one imaginary vibration (Figure 7) whose form describes the motion of atoms H_8 and H_{15} in order to form tautomers iC_{DW} and iC_{EW}. With the structure of the transition state we performed IRC calculations to get the ground-state energy curve of the thermal reaction – Figure 8. We found a drastic reduction of the energy barrier which is 0.662 eV (about 9 times) as compared to the mechanism discussed in Figure 6. Furthermore, we studied the excited-state paths over the thermal energy curve. It is clear that the water assisted proton transfer occurs photochemically along the $^1\pi\pi^*$ excited-state reaction path with a low energy barrier of 0.462 eV.

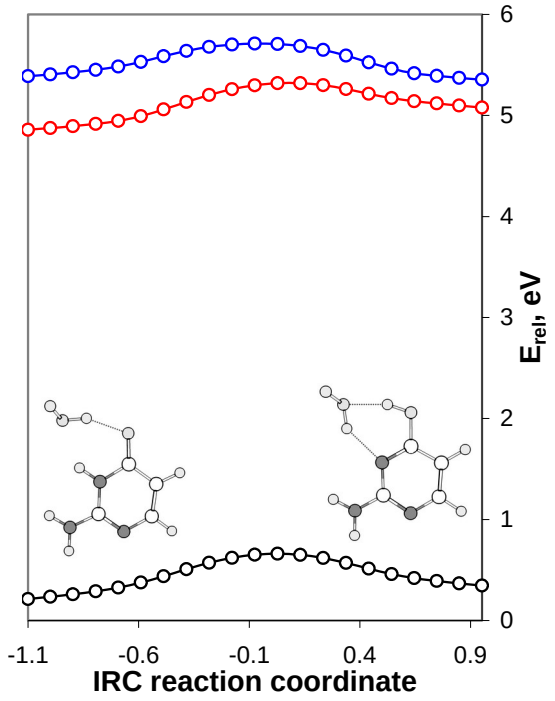

Figure 8: Excited-state reaction paths of the water assisted proton transfer $iC_{DW} \rightarrow iC_{EW}$ in water medium (PCM). The relative energy was calculated by the energy of the ground-state equilibrium geometry of the system iC_{DW} (-471.473381 a.u.).

No conical intersections between the energy curves are observed. We believe that this mechanism can explain the tautomeric conversion of isocytosine when irradiated with UV light.

5. CONCLUSION

The irradiation of aqueous solution of isocytosine with UVC light showed that a tautomeric photoconversion is a first order reaction with a rate constant of 5.29×10^{-3} min^{-1}. After removing the UV light source, we observed a dark reaction and a restoration of initial tautomer with a rate constant of

0.12×10^{-3} min^{-1}. The careful analysis of the UV absorption spectra of the irradiated and non-irradiated solution and the theoretically simulated UV spectra of several tautomers of isocytosine led to the conclusion that the photreaction is between the amino-oxo and amino-hydroxy tautomers of the compound. The mechanism of this oxo-hydroxy phototautomeris was studied at the B3LYP/aug-cc-pVDZ theoretical level in water surroundings according to PCM. We tested two principally different mechanisms – PIDA (24-28) and a water-assisted excited-state proton transfer. The first mechanism proposed a consecutive dissociation and association of N-H and O-H bonds through conical intersections S_0/S_1 which occur along the $^1\pi\sigma^*$ excited-state reaction pathway. The second mechanism, which we believe is the much more probable one, is supported by a water molecule and occurs along the $^1\pi\pi^*$ excited-state reaction pathway. This energy curve was found over the ground state IRC reaction pathway. The water molecule drastically reduces the energy barrier in the ground state as well in the excited state.

The findings here are important since they give an answer of the question why the nature “has chosen” cytosine for a pyrimidine base to be included in nucleic acid macromolecules instead of isocytosine.

6. CONFLICT OF INTEREST

We declare no conflict of interest.

7. ACKNOWLEDGMENTS

We would like to thank to the Bulgarian National Science Fund for the financial support of the research in the frames of the project No KP-06-N59/7. The authors gratefully acknowledge also: i) the Department of scientific research at the University of Plovdiv for administrating the project; ii) the provided access to the e-infrastructure of the NCHDC - part of the Bulgarian National Roadmap on RIs, with the financial support by the Grant No D01-168/28.07.2022.

7. REFERENCES

1. Callis PR. Electronic States and Luminescence of Nucleic Acid Systems. Annual Review of Physical Chemistry. 1983 Oct;34:329-28. Available from: <URL>.

2. Daniels MH, Hauswirth WW. Fluorescence of the purine and pyrimidine bases of the nucleic acids in neutral aqueous solution at 300 degrees K. Science 1971 Feb;171:675-2. Available from: <URL>.

3. Crespo-Hernandez CE, Cohen B, Hare PM, Kohler B. Ultrafast Excited-State Dynamics in Nucleic Acids. Chemical Reviews. 2004 Apr;104:1977-42. Available from: <URL>.

4. Cohen B., Crespo-Hernandez CE, Kohler B. Strickler–Berg analysis of excited singlet state dynamics in DNA and RNA nucleosides. Faraday Discussions. 2004 May;127:137-10. Available from: <URL>.

5. Shukla M., Leszczynski J. (Eds.). Radiation Induced Molecular Phenomena in Nucleic Acids, Springer,2008. ISBN: 978-1-4020-8183-5.

6. Rios AC, Tor Y. On the Origin of the Canonical Nucleobases: An Assessment of Selection Pressures across Chemical and Early Biological Evolution. Israel Journal of Chemistry. 2013 May;53:469-14. Available from: <URL>.

7. Hünig I, Plützer C, Seefeld KA, Löwenich D, Nispel M, Kleinermanns K. Photostability of Isolated and Paired Nucleobases: N-H Dissociation of Adenine and Hydrogen Transfer in its Base Pairs Examined by Laser Spectroscopy. ChemPhysChem 2004 Sep;5:1427-4. Available from: <URL>.

8. Egel R, Lankenau A, Mulkidjanian AY (Eds.). Origins of Life: The Primal Self-Organization, Berlin, Springer-Verlag, 2011. ISBN: 978-3-642-21624-4.

9. Dimitrov BH, Bakalska RI, Delchev VB. Phototautomerism of isocytosine in water medium: theoretical and experimental study. Journal of Structural Chemistry (Zhurnal Strukturnoi Khimii). 2019 Jan;60**:** 937-10. Available from: <URL>.

10. Bakalska RI, Delchev VB. Comparative study of the relaxation mechanisms of the excited states of cytosine and isocytosine. Journal of Molecular Modeling. 2012 Jul;18:5133-13. Available from: <URL>.

11. Merchan M, Gonzalez-Luque R, Climent T, Serrano-Andres L, Rodriguez E, Reguero M, Pelaez D. Unified Model for the Ultrafast Decay of Pyrimidine Nucleobases. The Journal of Physical Chemistry B 2006 Dec; 110:26471-5. Available from: <URL>.

12. Switzer C, Moroney SE, Benner SA. Enzymatic incorporation of a new base pair into DNA and RNA. Journal of the American Chemical Society. 1989 Oct;111:8322-1. Available from: <URL>.

13. Roberts C, Bandaru R, Switzer C. Theoretical and Experimental Study of Isoguanine and Isocytosine: Base Pairing in an Expanded Genetic System. Journal of the American Chemical Society. 1997 May; 119:4640-9. Available from: <URL>.

14. Edwards PD, Albert JS, Sylvester M, Aharony D, Andisik D, Callaghan O, Campbell JB, Carr RA, Chessari G, Congreve M, Frederickson M, Folmer RHA, Geschwindner S, Koether G, Kolmodin K, Krumrine J, Mauger RC, Murray CW, Olsson LL, Patel S, Spear N, Tian G. Application of Fragment-Based Lead Generation to the Discovery of Novel, Cyclic Amidine β-Secretase Inhibitors with Nanomolar Potency, Cellular Activity, and High Ligand Efficiency. Journal of Medicinal Chemistry. 2007 Nov;50:5912-13. Available from: <URL>.

15. Congreve M, Chessari G, Tisi D, Woodhead AJ. Recent developments in fragment-based drug discovery. Journal of Medicinal Chemistry. 2008 May;51:3661-19. Available from: <URL>.

16. Jeffrey GA, Kinoshita Y. The crystal structure of cytosine monohydrate. Acta Crystallografica. 1963; 16:20-8. Available from: https://doi.org/10.1107/S0365110X63000049.

17. McConnell JF, Sharma BD, Marsh RE. Co-crystallization of Two Tautomers: Crystal Structure of Isocytosine. Nature 1964 Jul;203:399-1. Available from: <URL>.

18. Morita H, Nagakura S. The electronic absorption spectra and the electronic structures of cytosine, isocytosine, and their anions and cations. Theoretica Chimica Acta 1968 Jan;11:279-16. Available from: <URL>. .

19. Dračínský M, Jansa P, Ahonen K, Buděšínský M. Tautomerism and the Protonation/Deprotonation of Isocytosine in Liquid- and Solid-States Studied by NMR Spectroscopy and Theoretical Calculations. European Journal of Organic Chemistry. 2011 Jan; 2011:1544-7. Available from: <URL>.

20. Raczyńska ED. On Analogies in Proton-Transfers for Pyrimidine Bases in the Gas Phase (Apolar Environment)—Cytosine Versus Isocytosine. Symmetry 2023 Jan;15:342. Available from: <URL>.

21. Brown DJ, Lyall JM. The Fine Structure of Cytosine. Australian Journal of Chemistry. 1962;15:851-6. Available from: <URL>.

22. Vranken H, Smets J, Maes G. Infrared spectra and tautomerism of isocytosine; an ab initio and matrix isolation study. Spectrochimica Acta A 1994 May;50:875-14. Available from: <URL>.

23. Nowak MJ, Lapinski L, Fulara J. Matrix isolation studies of cytosine: The separation of the infrared spectra of cytosine tautomers. Spectrochim Acta A 1989;45:229-13. Available from: <URL>.

24. Chmura B, Rode M, Sobolewski AL, Lapinski L, Nowak M. A Computational Study on the Mechanism of Intramolecular Oxo−Hydroxy Phototautomerism Driven by Repulsive πσ* State. The Journal of Physical Chemistry A 2008 Dec;112:13655-6. Available from: <URL>.

25. Sobolewski AL, Domcke W. The chemical physics of the photostability of life. Europhysics News 2006 Oct;37:20-3. Available from: <URL>.

26. Perun S, Sobolewski A, Domcke W. Conical intersections in thymine. The Journal of Physical Chemistry A 2006 Nov;110:13238-6. Available from: <URL>.

27. Delchev VB, Sobolewski AL, Domcke W. Comparison of the non-radiative decay mechanisms of 4-pyrimidinone and uracil: an ab initio study. Physical Chemistry Chemical Physics. 2010 Apr;12:5007–8. Available from: <URL>.

28. Delchev VB, Ivanova IP. Theoretical study of the excited-state reaction paths of the OH- and NH-dissociation processes in barbituric acid. Monatsh Chem. 2012 May;143:1141-9. Available from: <URL>.

29. Becke AD. Density-functional thermochemistry. III. The role of exact exchange. Journal of Chemical Physics. 1993 April; 98:5648-4. Available from: <URL>.

30. Lee C, Yang W, Parr RG. Development of the Colle-Salvetti correlation-energy formula into a functional of the electron density. Physical Review B. 1988 Jan ;37:785-4. Available from: <URL>.

31. Hättig C, Weigend F. CC2 excitation energy calculations on large molecules using the resolution of the identity approximation. The Journal of Chemical Physics. 2000 Oct;113:5154-7. Available from: <URL>.

32. Bauernschmitt R, Ahlrichs R. Treatment of electronic excitations within the adiabatic approximation of time dependent density functional theory. Chem Phys Lett. 1996 July; 256:454-10. Available from: <URL>.

33. Stratmann RE, Scuseria GE, Frisch MJ. An efficient implementation of time-dependent density-functional theory for the calculation of excitation energies of large molecules. J Chem Phys. 1998 Nov; 109:8218-6. Available from: <URL>.

34. Miertuš S, Scrocco E, Tomasi J. Electrostatic Interaction of a Solute with a Continuum. A Direct Utilization of ab initio Molecular Potentials for the Prevision of Solvent Effects. Chem Phys. 1981 Feb; 55:117-12. Available from: <URL>.

35. Frisch MJ, Trucks GW, Schlegel HB, Scuseria GE, Robb MA, Cheeseman JR, et al. Gaussian˜16 Revision C.01. Wallingford, CT: Gaussian, Inc.; 2016.

36. Barca GMJ, Bertoni C, Carrington L, Datta D, De Silva N, Deustua JE, Fedorov DG et al. Recent developments in the general atomic and molecular electronic structure system. The Journal of Chemical Physics. Sep 2020; 152: 154102. Available from: <URL>.